EIC Detector R&D Progress Report

Project ID: eRD14

Project Name: PID Consortium for an integrated program for Particle Identification (PID) at a future Electron-Ion Collider

Period Reported: from 7/1/2016 to 12/31/2016

Contact Persons: Pawel Nadel-Turonski and Yordanka Ilieva

Project Members:

M. Alfred[9], L. Allison[15], M. Awadi[9], B. Azmoun[3], F. Barbosa[13], W. Brooks[17], T. Cao[18],

M. Chiu[3], E. Cisbani[11,12], M.Contalbrigo[10], A. Datta[19], A. Del Dotto[11,20], M. Demarteau[2],

J.M. Durham[14], R. Dzhygadlo[8], D. Fields[19], Y. Furletova[13], C. Gleason[20],

M. Grosse-Perdekamp[18], J. Harris[6], X. He[7], H. van Hecke[14], T. Horn[4],

J. Huang[3], C. Hyde[15], Y. Ilieva[20], G. Kalicy[4], M. Kimball[1], E. Kistenev[3], Y. Kulinich[18],

M. Liu[14], R. Majka[6], J. McKisson[13], R. Mendez[14], P. Nadel-Turonski[16], K. Park[13],

K. Peters[8], T. Rao[3], R. Pisani[3], Yi Qiang[13], P. Rossi[13], M. Sarsour[7],

C. Schwarz[8], J. Schwiening[8], C.L. da Silva[14], N. Smirnov[21], H. Stien[1], J. Stevens[5],

A. Sukhanov[3], S. Syed[7], A. Tate[1], J. Toh[18], C. Towell[1], R. Towell[1], T. Tsang[3], R. Wagner[2],

J. Wang[2], C. Woody[3], C.-P. Wong[7], W. Xi[13], J. Xie[2], Z.W. Zhao[6], B. Zihlmann[13], C. Zorn[13].

[1] Abilene Christian University, Abilene, TX 79601

[2] Argonne National Lab, Argonne, IL 60439

[3] Brookhaven National Lab, Upton, NY 11973

[4] Catholic University of America, Washington, DC 20064

[5] College of William & Mary, Williamsburg, VA 2318

[6] Duke University, Durham, NC 27708

[7] Georgia State University, Atlanta, GA 30303

[8] GSI Helmholtzzentrum für Schwerionenforschung GmbH, 64291 Darmstadt, Germany

[9] Howard University, Washington, DC 20059

[10] INFN, Sezione di Ferrara, 44100 Ferrara, Italy

[11] INFN, Sezione di Roma, 00185 Rome, Italy

[12] Istituto Superiore di Sanità, 00161 Rome, Italy

[13] Jefferson Lab, Newport News, VA 23606

[14] Los Alamos National Lab, Los Alamos, NM 87545

[15] Old Dominion University, Norfolk, VA 23529

[16] Stony Brook University, Stony Brook, NY 11794

[17] Universidad Técnica Federico Santa María, Valparaíso, Chile

[18] University of Illinois, Urbana-Champaign, IL 61801

[19] University of New Mexico, Albuquerque, NM 87131

[20] University of South Carolina, Columbia, SC 29208

[21] Yale University, New Haven, CT 06520

Abstract

Excellent particle identification (PID) is an essential requirement for a future Electron-Ion Collider (EIC) detector. Identification of the hadrons in the final state is needed for understanding how different quark flavors contribute to the properties of the nucleon, and reliable identification of the scattered electron is important for covering kinematics where pion backgrounds are large. The EIC PID consortium (eRD14) was thus formed to develop an integrated PID program using a suite of complementary technologies covering different ranges in rapidity and momentum, as required by the asymmetric nature of the collisions at the EIC. The PID consortium has also worked closely with BNL and JLab to ensure that the specific R&D projects are compatible with the detector concepts that are being pursued there.

Table of Contents

1. Introduction

Identification of hadrons in the final state is essential for key EIC measurements formulated in the EIC White Paper and referenced in the NSAC Long Range Plan. These include 3D imaging of the nucleon in momentum space through semi-inclusive DIS, where flavor tagging can tell us about the transverse momentum distributions (and potentially orbital angular momentum) of the strange sea, and open charm (with decays of D-mesons into kaons) which is important for probing the distribution of gluons in protons and nuclei.

Satisfying the PID requirements within the very asymmetric kinematics of the EIC (discussed in detail in the eRD14 proposal for FY17) requires a suite of detector technologies addressing the specific challenges (in terms of momentum coverage, space, etc) encountered in various ranges of rapidity. The integrated PID program pursued by the eRD14 consortium thus includes different detector systems for each endcap and the central barrel, as well as corresponding sensor and readout solutions. While compatibility is ensured with the central detector concepts developed at BNL and JLab, all funded R&D being pursued by the consortium is conceptually novel. The dual-radiator RICH (dRICH) for the hadron endcap is the first such design for a solenoid-based collider detector. The modular aerogel RICH (mRICH) for the electron endcap introduces lens-based focusing, which improves momentum coverage and reduces the required detector volume and sensor area compared with state-of-the-art. The very compact, high-performance DIRC for the barrel combines new optics for spatial imaging with timing to allow a significant improvement in momentum coverage compared with the state-of-the-art. The funded work on photosensors in high magnetic fields and adaptation of LAPPDs to EIC requirements is also aimed at developing a new generation of devices.

In order to be able to coherently evolve the 1integrated concept, the consortium goals for FY17 were to demonstrate in simulation the possibility of making a dRICH satisfying the constraints of the proposed EIC detector(s); to verify the simulations for the mRICH by comparing photon yields with initial test beam data and to prepare for a beam test in a configuration with longer focal length and smaller pixels to demonstrate the PID performance of the lens-based concept; to evaluate the advanced DIRC optics in test beam data and on the test bench, and find the best ways to fold in timing into the design and reconstruction. We also wanted to conduct a follow-up high-B sensor measurement at JLab, but also understand possible synergies with the new facility at ANL for future measurements, which will be used to test the LAPPDs. To make the necessary progress in all these areas, the some adjustments were made to the consortium budget for FY17 (including no-cost extensions of FY16 funding). In addition to the funded work, externally funded efforts have continued on high-resolution TOF, and we are preparing a broader for effort for readout electronics, also involving the Hawaii group. In this report we summarize the progress for since the submission of the FY17 proposal.

2. Hadron Identification

2.1 Summary

The funded R&D on the three Cherenkov systems has been proceeding well, and they all promise significant advances over the fallback options (single-radiator gas RICH for the dRICH, proximity-focusing aerogel RICH for the mRICH, or a DIRC geared only towards spatial imaging). The mRPC-based high-resolution TOF was not funded in FY17, but with work has continued with external funding. Since this technology is considered both for the SoLID detector at JLab and sPHENIX at BNL, developments remain relevant for the EIC PID consortium.

2.2 Dual-Radiator RICH (dRICH)

The goal of the dRICH detector is to provide good hadron separation (π/K/p) up to 50 GeV/c, in the forward, ion-side region of the EIC detector.

2.2.1 Past

2.2.1.1 What was planned for this period?

The plan was to evaluate different focusing geometries and radiator combinations using semi-analytical models. As in the case of LHCb and HERMES, a dual-radiator RICH with outward-reflecting mirrors was found to be the best overall solution, but the combination and integration of the radiators as well as the layout and mirror geometry had to be quite different to fit the requirements of a solenoid-based detector in general and the EIC requirements in particular (space, B-field, and momentum coverage). The evaluation was based on a GEANT4 simulation (using the GEMC framework). Particular attention was paid to finding a geometry which allowed a common sensor to be used for both radiators and minimised the sensor area, since the latter is the main cost driver for this type of detector. Another consideration was to reduce the radiation exposure of the photosensors, which was addressed by a solution where the outward-reflecting mirrors allowed placing the sensors far away from the beam and in the shadow of a barrel calorimeter (as seen from the collision point). An additional advantage of this arrangement is that the sensors do not take up any of the longitudinal space available - which is restricted in the EIC due to luminosity requirements. The effort for the fall of 2016 was focusing on a geometry based on the space allocated in the JLab detector concept, while the feasibility of more compact configurations more suitable with the current layout of the BNL endcap designs will be pursued in the spring. These studies are benefiting from the experience of several groups that have built similar devices in the past, and also by the experience from the construction of the CLAS12 RICH, which is in progress [1,2,3].

2.2.1.2 What was achieved?

All the goals were achieved and work is on track as planned. Simulations were initially performed for a configuration using aerogel (n=1.02) and CF_4 gas, but this does not provide continuous momentum coverage in imaging mode, *i.e.*, without the need to use the gas radiator as a threshold device to cover an intermediate region. However, the study showed that this complication can be avoided by replacing CF_4 with C_2F_6. The key parameters for the latter configuration were: i) device length 1.65 m; ii) aerogel radiator (n(400 nm) = 1.02); thickness 4 cm; iii) C_2F_6 gas tank length 1.6 m; iv) polar angle coverage [5°,25°]; v) mirror radius 2.9 m. The detector is made of six identical sectors, each covering an azimuthal angle of 60°, as shown in Fig. 2.2.1. The 3D focusing possible in a sectorized configuration reduces size of the the sensor area on the focal plane.
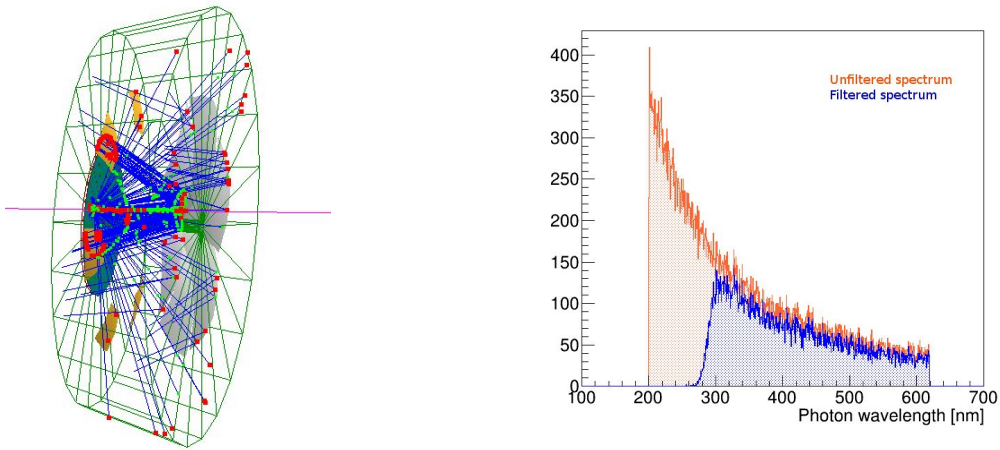
Figure 2.2.1: (Left panel)The GEMC based simulation of the dRICH. In transparent red is the aerogel radiator (the acrylic filter is in front), in transparent green is the gas radiator volume; the mirrors sectors are in gray and the photo-detector surfaces (spherical shape) of about 8500 cm^2 per sector in dark-yellow. A pion event of momentum 10 GeV/c is simulated. Emitted optical photons are in blue. (Right panel) The effect of the acrylic filter on the emitted photons spectrum is shown.

The properties of the aerogel (n=1.02) used for the simulation were based on detailed studies carried out by the CLAS12 RICH collaboration [3] for currently available aerogel. In particular, the absorption length and effects due to Rayleigh scattering, the latter being one of the main sources of background and optical dispersion, were included in the GEMC simulation.

To avoiding chemical corruption of the aerogel and to filter photons with wavelength below 300 nm (a region in which the Rayleigh scattering is sizable), a 3-mm-thick acrylic shield was added to separate the aerogel from the gas.

Since the dRICH will operate in a non-negligible magnetic field, the charged particle tracks will bend as they pass through the gas radiator (the effect is small in the thin aerogel). This gives an additional source of uncertainty on the Cherenkov ring reconstruction. The effects of the magnetic field have been incorporated in the simulation and reconstruction. Initially, the 3T field

map of JLab detector design was used, but simulations will also be carried out with field maps from the ePHENIX and BeAST.

In the simulations, the pixel size of the photosensors is assumed to be of 3 mm and the QE curve follows that of the Hamamatsu H12700 multi-anode PMT. The reconstruction of the Cherenkov angle is based on the indirect ray tracing algorithm used by the HERMES experiment (see [1] for details on the algorithm). The two upper plots of Fig. 2.2.2 show the main error contributions to the single p.e. angular resolution of the two radiators as a function of the charged particle track polar angle. The effect of the momentum and angular resolution of the particles track have been also taken into account and considered as one of the single p.e. angular error source. The bottom plot of Fig. 2.2.3, shows the PID performances for particles of polar angle of 15°.
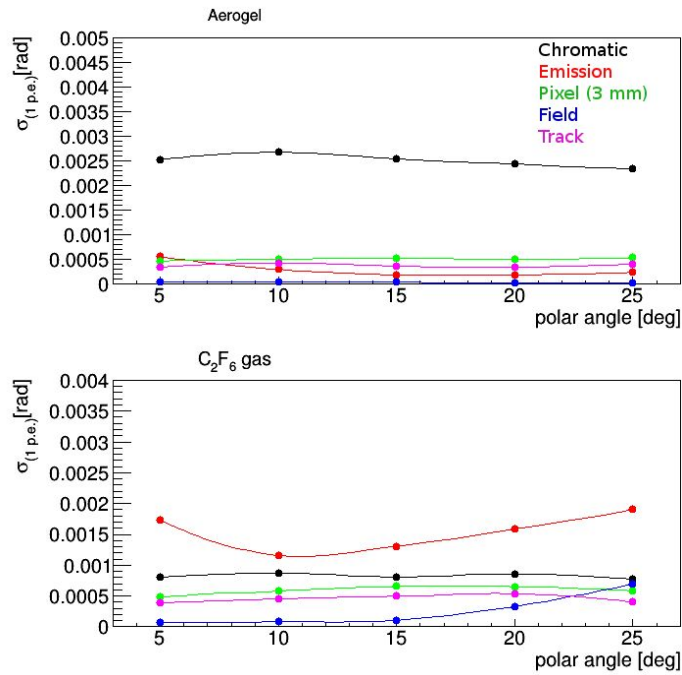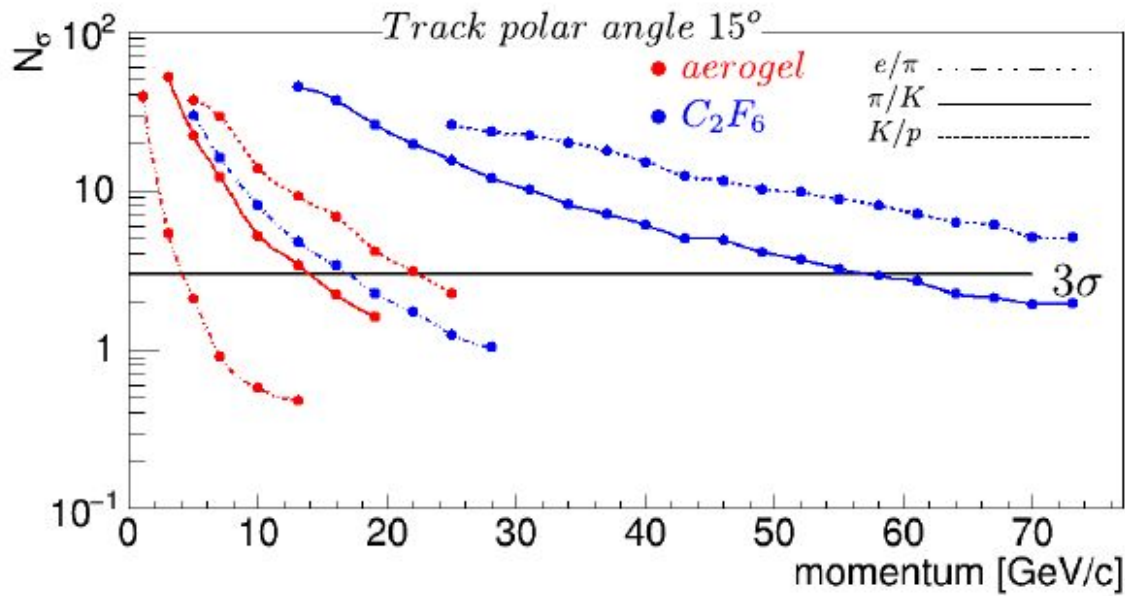
Figure 2.2.2: (Upper two plots) dRICH single p.e. angular error sources, assuming a pixel size of 3 mm and an angular uncertainty on the track direction of 0.5 mrad. (Lower plot) Particle separation power (in terms of the number of sigmas) for tracks with 15° polar angle.

2.2.2 Future

2.2.2.1 What is planned for the next funding cycle and beyond? How, if at all, is this planning different from the original plan?

The plan for the next funding cycle and beyond has three elements: 1) to further evolve the simulation to resolve outstanding questions, 2) extend the simulations to explore performance of more compact configurations currently considered at BNL (and comparison with single radiator RICH alternatives), and 3) preparation for testing key issues in a small-scale prototype. This follows our original plan and the recommendations of the committee. The plan includes:

- A more detailed study of the optical background, also adding the acrylic shield mentioned above.
- Study and implementation of existing (or new) reconstruction algorithms to be compared with the IRT algorithm.
- GEMC-based digitalization of the photodetector (also useful for the definition of the photon detector baseline), optimal pixel shape to fit with a non planar surface.
- Formulation of requirements on the EIC detector for optimal RICH performance (magnetic field, track reconstruction, etc).
- Simulation of the feasibility of a compact version of the dRICH to better fit the BNL versions of the EIC detector, and evaluate the performance using the current BNL parameters for the magnetic field.

- Identification of baseline candidates as a magnetic field tolerant photon detectors (MCP-PMT, SiPM (both on the market) and LAPPD).
- Study and definition of a first prototype.

2.2.2.2 What are the critical issues?

The critical issue for the development of the dRICH is to ensure that it can work properly within the constraints of the EIC detector - in particular in terms of space and magnetic field. For the latter, it is crucial to find a design with an optimal integration with appropriate (and affordable) photosensors. This requires more detailed simulations (*e.g.*, digitalization of the photosensors in GEMC) in synergy with the hardware activities leading to a validation through the construction of a prototype.

References:

[1] Akopov, Norair, et al. "The HERMES dual-radiator ring imaging Cherenkov detector." NIMA 479.2

(2002): 511530.

[2] Adinolfi, M., et al. "Performance of the LHCb RICH detector at the LHC." Eur. Phys. J. C 73.5 (2013): 117; Alves Jr, A. Augusto, et al. "The LHCb detector at the LHC." Journal of instrumentation 3.08 (2008): S08005; Nobrega, R. Antunes, et al. "LHCb reoptimized detector design and performance: Technical Design Report." (2003): x127.

[3] Anefalos Pereira., et al. "Test of the CLAS12 RICH large scale prototype in the direct proximity focusing configuration.", Eur. Phys. J. A 52 (2016).

[4] A. Del Dotto for the EIC PID consortium, "Design and R&D of RICH detectors for EIC experiments "presented at RICH 2016, 9th International Workshop on Ring Imaging Cherenkov Detectors; (proceedings will be published in NIMA).

2.3 Modular aerogel RICH

The goal of the modular aerogel RICH (mRICH) is to provide hadronic PID capability with momentum coverage from 3 to 10 GeV/c with a compact design in order to overcome the space limitations of the EIC experiments. Although the multi-layer proximity-focusing RICH design, such as ARICH at BELLE2 [1], can achieve three-sigma K/π separation at 4 GeV/c, a larger expansion volume is required for PID in higher momentum range.

A multi-layer proximity-focusing RICH design increases PID separation power by increasing number of detected photons (N_γ) by adding successive layers of radiator while keeping the uncertainty of Cherenkov angle (σ_θ) of single photon measurement. In contrast, the novel lens-based mRICH design improves the separation power by minimizing the uncertainty σ_θ as a result of lens focusing, as shown in Figure 2.3.1 (right), which also requires a smaller coverage of the photosensor plane.
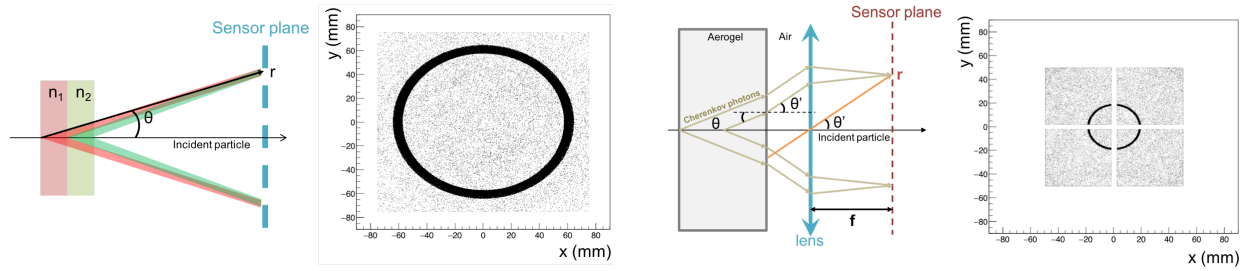
Figure 2.3.1: Ray diagrams (not to scale) and the Geant4 simulation results of the BELLE-2 ARICH detector design (right) and the mRICH lens-based detector design (left). The ring images are generated from 100 9-GeV/c pions in both cases. The distance from the sensor plane of the proximity RICH to the mid-point of n_1 and n_2 is 20 cm. The total thickness of n_1 and n_2 is 4 cm. The focal length of the mRICH Fresnel lens is 7.6 cm and the mRICH aerogel block thickness is 3.3 cm.

The mRICH detector design is shown in Figure 2.3.2 together with an event display of a 9 GeV/c pion using Geant4 simulation. The first mRICH prototype consists of a 3.3cm thick aerogel block with refractive index 1.03, a Fresnel lens (3-inch focal length), a four-sided (top, bottom, left and right) mirror set, and a sensor plane covered by four Hamamatsu 12700A photomultiplier arrays.
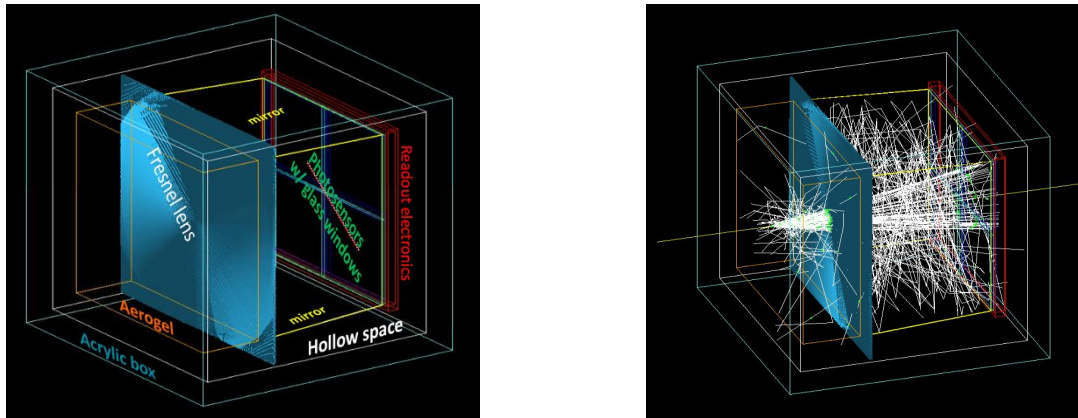
Figure 2.3.2: mRICH detector design (left) and an event display (right) from a 9 GeV/c pion using Geant4 simulation.

2.3.1 Past

### 2.3.1.1 What was planned for this period?

The work planned for this period included: 1) analyzing the first mRICH test beam data and preparing for publication of the results; 2) optimizing the choice of the Fresnel lens focal length; and 3) improving the detector design and building the second mRICH prototype.

2.3.1.2 What was achieved?

Test Beam Data Analysis

The first prototype beam test was performed at Fermilab in April of 2016. The beam test data has been analyzed to demonstrate the detector working principle by comparing the Cherenkov ring image properties including ring radius, center position and number of photons detected against the realistic Geant4 simulation results.

An event-by-event ring reconstruction analysis, using a Circular Hough Transform algorithm, is performed both for the simulated and test beam data. Figure 2.3.3 shows the reconstructed Cherenkov ring images from the data and the Geant4 simulation.
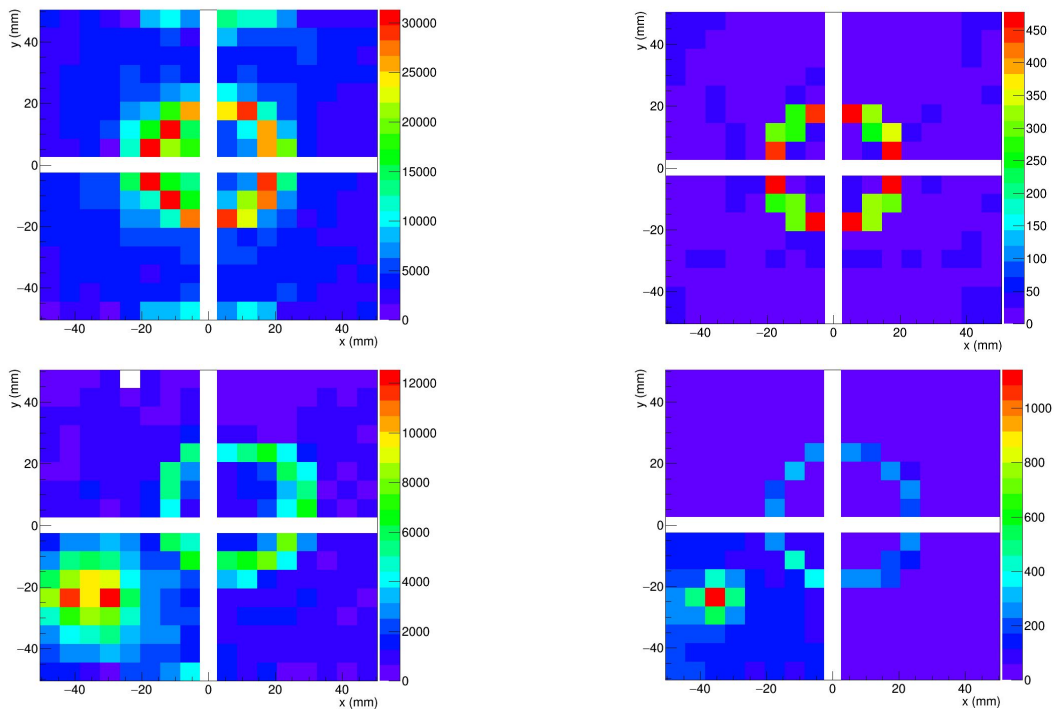
Figure 2.3.3: Accumulated ring image displays: (top-left) from the 120 GeV proton beam incident toward the center of the mRICH; (top-right) from the matching Geant4 simulations. The blank regions are the gaps between the four Hamamatsu H12700 modules. The bottom-left is the ring image display from the 120 GeV/c proton beam incident toward the lower-left quadrant of the mRICH and the bottom-right is the corresponding image display from Geant4 simulation.

The analysis was focused on the data set taken from the 120 GeV/c primary proton beam because of its smaller beam size, in order to quickly verify the detector working principle and validate the Geant4 simulation results by comparing the ring radius and the number of Cherenkov photons. The analysis results are summarized in Table 2.3.1. A draft of a NIM A paper about the beam test results is currently under circulation for comments within the eRD14 Consortium.

	Analytical Calculation	Test Beam Data	Geant4 Simulation
Ring Radius (mm)	19.4	19.0±1.3	18.9±1.0
# of photon per event	10.4	11.0±2.9	11.1±2.9

Table 2.3.1: Summary of the ring radii and the number of Cherenkov photons from the 120 GeV/c primary proton beam incident toward the center of the mRICH detector.

Optimization Study of the Fresnel Lens Focal Length

Given the remarkable consistency of the results from the beam test data and from the Geant4 simulation, extensive simulations have been carried out for optimizing the choices of the Fresnel focal length for the best PID performance of the mRICH detector. The results from these simulation studies are shown in Fig. 2.3.4.
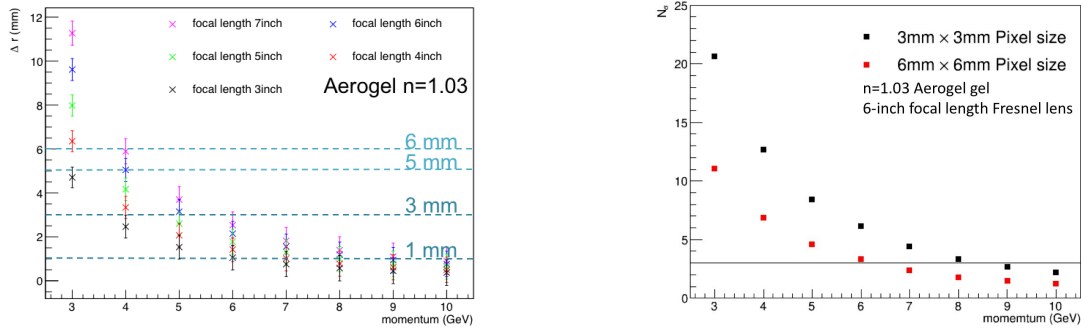
Figure 2.3.4: Simulation results of the mRICH PID performance as a function of particle momentum. (Left panel) The difference of ring radii (Δr) from pion and kaon rings with different Fresnel lens focal lengths. (Right panel) The PID separation power of the mRICH design (with 6-inch focal length Fresnel lens) for two choices of the photon sensor pixel size. [Note: for the first beam test, Hamamatsu H12700 multi-anode PMT (6mm x 6mm pixel size) was used.]

2.3.1.3 What was not achieved, why not, and what will be done to correct?

There is no progress of studying the mRICH performance in the context of the EIC experiments. The main reason is the lack of manpower support for carrying out this study. We are also seeking funding support from Georgia State University to build the second prototype and to run the next beam test.

2.3.2 Future

2.3.2.1 What is planned for the next funding cycle and beyond? How, if at all, is this planning different from the original plan?

- Publish the results from the first mRICH prototype beam test (top priority).
- Build the second mRICH prototype with a 6-inch focal length Fresnel lens and 3mm×3mm pixel size photosensors (i.e., Hamamatsu H13700).

- Implement the mRICH design in fsPHENIX [2] and ePHENIX [3] in the forward rapidity region.

2.3.2.2 What are the critical issues?

While we are grateful to the effort from the INFN group (led by Marco Contalbrigo) for providing the DAQ system of the first beam test without any funding from the EIC R&D, the detector readout for the second prototype beam test will be one of the critical issue in order to read out over 1000 channels from four H13700 modules.

References

[1] E. Torassa, "Particle identification with the TOP and ARICH detectors at Belle II", NIM A, 824 (2016): 152.

[2] J. Seele, "The sPHENIX Forward Upgrade (and ePHENIX)", Nuclear Physics A, 904 (2013): 933c.

[3] B. Jacak, "The next decade of physics with PHENIX", Nuclear Physics A, 855.1 (2011): 514.

2.4 High Performance DIRC

A radially-compact detector based on the DIRC (Detection of Internally Reflected Cherenkov light) principle is a very attractive solution for EIC, providing particle identification (e/π, π/K, K/p) over a wide momentum range. The DIRC is a type of RICH detector using rectangular-shaped radiators made of synthetic fused silica that also function as light guides transporting the Cherenkov photons to an expansion volume, where they are recorded by an array of photon sensors. During the photon transport the emission angle of Cherenkov photons with respect to the particle track is maintained and can be reconstructed from the measured parameters. DIRC detectors are inherently 3D devices, measuring the image location on the detector surface (*x, y*) and the time of arrival of each photon (*t*).

The High Performance DIRC design developed for the EIC detector is inspired by the original DIRC detector, used by BaBar, and the PANDA Barrel DIRC detector, currently in development. The baseline design, implemented in a Geant4 simulation, is shown in Fig. 2.4.1a. The radiators each are 4.2 m long, with a cross-section of 17 mm x 32 mm. Eleven such bars are placed side-by-side, separated by a small air gap, into a bar box. The 16 bar boxes are arranged in a barrel with a radius of 1 m around the beam line. Mirrors are attached to one end of each bar. On the opposite end, where photons exit the bar, a special 3-layer spherical lens is attached to each bar. The other side of the 3-layer lens is coupled to a large prism-shaped expansion volume, made of synthetic fused silica. A closeup view of this region is shown in Fig. 2.4.1b. The prism has a 38° opening angle, and the dimensions 285 mm x 390 mm x 300 mm. The detector plane of each prism is covered by 2 mm x 2 mm pixels for a total of about 450k channels to record the location and arrival time of the Cherenkov photons.

A key component to reach the required performance is a special 3-layer spherical compound lens. A schematic and photos of a prototype lens, tested in 2015, are shown in Fig. 2.4.1c. This lens contains a layer of the high-refractive index material Lanthanum crown glass (NLaK33), sandwiched between two layers of synthetic fused silica. The two radii of the 3-layer lens were optimized to remove aberrations present in standard lenses by first defocusing and then focusing the photons to create a flat focal plane, matching the geometry of the prism expansion volume.
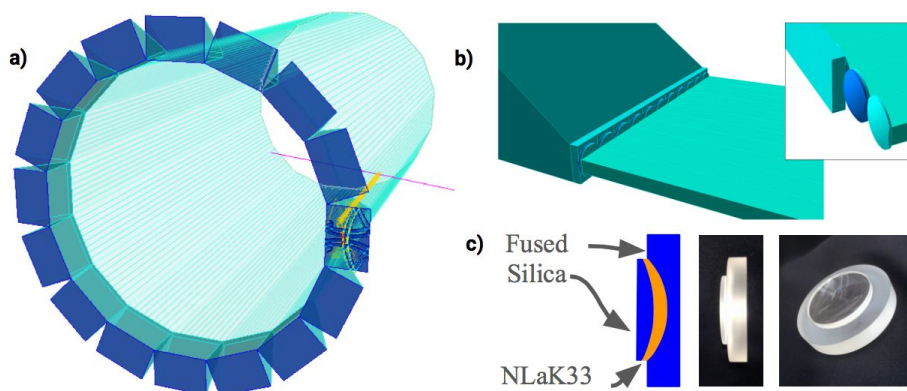
Figure 2.4.1: a) Geant4 geometry for the simulation of the high-performance DIRC. b) The fused silica prism expansion volume, a row of spherical three-layer lenses with high index of refraction (no air gaps) and the radiator bars. The insert shows the individual lenses and layers of the spherical lens system. c) Schematic and photos of the 3-layer lens prototype.

2.4.1 Past

2.4.1.1 What was planned?

The key hardware-related activity planned for FY17 is to determine the performance of a spherical 3-layer lens on test benches and with particle beams. Results of these tests are crucial to complete the design and procurement of the radiation-hard cylindrical 3-layer lens prototype.

Simulation activities focus this year on the time-based imaging reconstruction method, finishing its development, using it for the cost/performance optimization of the bar/plate-based designs, and to identify the baseline design. Additional goals are: Determination of the optimum pixel size for the sensors and the time resolution requirement for the high-performance DIRC using time-based imaging; Investigation of the chromatic dispersion mitigation in the context of different photocathode materials (for the narrow bar geometry); Study the potential use of the DIRC for high-precision event timing.

2.4.1.2 What was achieved?

Experimental validation of the performance of the innovative 3-layer lens is crucial for the DIRC in the EIC R&D program. Pictures of the first prototype spherical lens are shown in Fig. 2.4.1. All

the hardware activities are focused on the study and validation of the properties of the prototype 3-layer lens. This includes measurements on test benches and in particle beam as part of the full-size prototype. Not all of the required components of the high-performance DIRC baseline design are available yet (such as sensors with small pixels, fast readout electronics, full-size radiators, etc.). However, the collaboration with the PANDA DIRC group provided an opportunity to evaluate the performance of the 3-layer spherical lens in a real particle beam experiment.

The modular design of the PANDA Barrel DIRC prototype allowed for the easy exchange of several components between measurements to test their impact on the prototype performance. Several types of radiators, lenses, and imaging options were tested during the 2015 and 2016 test beam campaigns at CERN. Due to the larger pixel size of the MCP-PMTs available for the test beam (6.5mm pixel pitch), the different length of the bar and size of the prism, the results from this test beam are not expected to agree with the performance predicted for the high-performance DIRC. However, the EIC DIRC simulation package can be used to translate the achieved performance to the EIC DIRC geometry.


2015 test beam at CERN: data analysis

The analysis of the data collected during the 2015 CERN test beam was continued and is close to completion. The analysis includes a detailed error evaluation and a new per-sensor calibration of the Cherenkov angle. The difference between the expected and reconstructed Cherenkov angle per photon is calculated for each MCP-PMT. Applying the shift of the mean value from zero to the experimental data improves the single photon Cherenkov angle resolution by 1-2 mrad.

2016 test beam at CERN

The test beam at CERN in October 2016 was primarily focused on the validation of the PID performance of the geometry using wide radiator plates, with and without a cylindrical lens. In addition, some time was dedicated to measurements with the narrow bar and the 3-layer spherical lens. A picture of the setup used at CERN with the wide plate is shown in Fig. 2.4.3a. The radiator plate was coupled to the cylindrical 2-layer lens or directly to the synthetic fused silica prism expansion volume with a 30° opening angle. The data analysis is still in the early stages but a preliminary result for the geometry with the wide plate and the 2-layer lens is shown in Fig. 2.4.3b. One should note that this result is obtained with a preliminary calibration and that the performance parameters are expected to improve with a more advanced analysis.
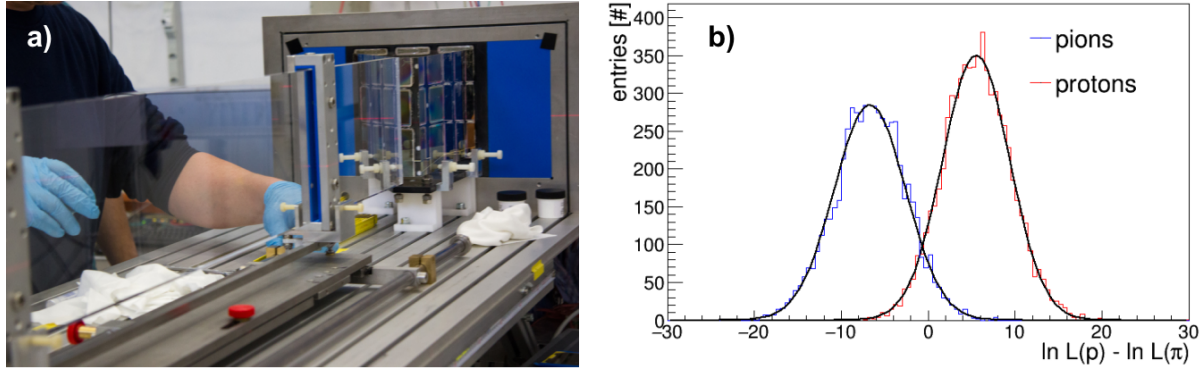
Figure 2.4.3: Photo of the PANDA Barrel DIRC 2016 prototype with the wide radiator plate (a). Preliminary result of the log-likelihood difference calculated using time-based imaging for proton and pion hypotheses for a sample of 7 GeV/c pions and protons at a 25° polar incidence angle for the wide plate and the 2-layer cylindrical lens (b). The π/p separation power extracted from the Gaussian fits is 3.1 standard deviations (s.d.) at 7 GeV/c, corresponding to 3.2 π/K s.d. at 3.5 GeV/c.

Mapping the focal plane of the 3-layer spherical at ODU

The schematic of the setup designed and built in the Old Dominion University laser lab to measure the shape of the focal plane of the 3-layer lens is shown in Fig. 2.4.4a. The lens was placed on a rotating stage and rotated through two parallel laser beams. The intersection point of the two laser beams determined the focal length. The lens was placed inside a 30 x 40 x 60 cm^3 glass container filled with mineral oil (with a refractive index very close to fused silica) to simulate the focusing behavior of the lens placed between the bar and the prism. The 3-layer lens is supported in a special 3D-printed holder that makes it possible to map out the focal plane in all three dimensions, which will be particularly important for comparing spherical and cylindrical lens designs. Preliminary results of that measurements and the prediction from the GEANT4 simulation are shown in Fig. 2.4.4b. Although systematic studies and additional measurements for other lens tilt angles are still in progress, it can be seen that the simulation agrees quite well with the experimental data and that the spherical lens produces the desired flat shape of the focal plane.
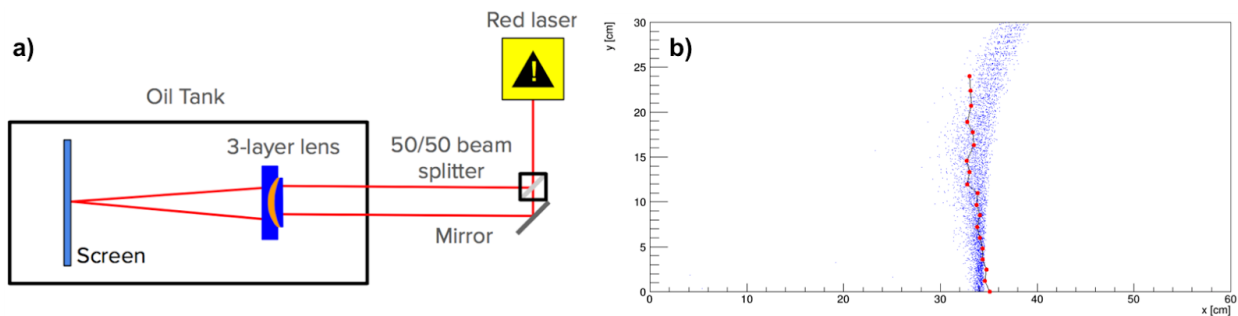
Figure 2.4.4: Schematic of the setup at ODU to map the shape of the 3-layer lens focal plane (a). Measured shape of the focal plane (red points) compared to simulation (blue points). The x coordinate corresponds to the focal length and the y coordinate to the focal point location perpendicular to the incident beams, calculated for different lens rotation angles. The spread of the simulation points reflects the size of the laser beam.

2.4.1.3 What was not achieved?

The radiation hardness measurement of the 3-layer lens at CUA was delayed due to technical issues with the X-Ray machine. All preparation work was completed: the required holders and additional samples of NLaK33 material and synthetic fused silica are ready for the measurement. By measuring the pure material samples separately the compound lens, potential damage to glue and coating can be distinguished from bulk damage effects. The fused silica sample will be serve as a reference in the monochromator used to measure transmission of the samples after each irradiation step. The repair of the X-Ray machine was completed at the end of December and the radiation tests are now scheduled for January.

Radiation hardness of the NLaK33 material will be crucial for the final decision of the design of the next 3-layer lens prototype. The procurement of the new cylindrical lens is planned for February to have it ready for the next test beam at the CERN PS, planned for summer 2017.

Development of the time-based imaging reconstruction method started but the hardware-related activities had higher priority in the first part of FY17. The work on the baseline design and pixel size study had to be delayed. Instead, we used the synergy with PANDA to evaluate the plate geometry with particle beams at CERN.

2.4.2 Future

2.4.2.1 What is planned for the rest of FY17? How, if at all, is this planning different from the original plan?

The PID@EIC consortium activities were re-prioritized after the report of the July 2016 Advisory Committee Meeting was received. The funding for the high-performance DIRC sub-project was cut by 50% compared to the budget application. As a result, the strategy and milestones for the high-performance DIRC R&D were reevaluated.

In terms of hardware, the procurement of the next-generation 3-layer cylindrical lens has the highest priority. This allows us to make the best use of the synergy with the PANDA Barrel DIRC beam test, expected in the summer of 2017, which is funded via external sources at GSI. To receive the lens in time it will be produced using the NLaK33 material, which is potentially not radiation hard but affordable within the reduced budget.

The measurements of the lens properties at ODU and CUA will continue as planned since no new procurement is required and the manpower is funded through external sources. This includes the analysis of the radiation hardness of the 3-layer lens and the NLaK33 sample. Furthermore, the 3D focal plane measurements will be completed by performing several additional measurement series and a detailed error evaluation.

The activities on the detailed GEANT simulation and the time-based imaging had to receive a lower priority since the budget did not provide funding for a new PostDoc. The work will be distributed in part to GSI, in particular the simulation of the new 3-layer cylindrical lens and improvements to the time-based imaging method. Additional work, like the optimization of the design in simulation, the mitigation of the chromatic errors, and the event timing, may have to be postponed to the next funding year.

2.4.2.2 What are the critical issues?

The optimization of the baseline design of the high-performance DIRC, including a comparison of the PID performance of the bar and plate geometries for the radiators, a study of the optimum sensor pixel size, and ways to mitigate effects of chromatic dispersion.

2.5 High Resolution Time-of-Flight

The high resolution TOF R&D aims to demonstrate that a 10 picosecond TOF system could be considered for particle identification at the EIC. Two detector technologies are investigated, multi-gap Resistive Plate Chambers (mRPC) and Micro-Channel Plate PMTs (MCP-PMT). In detector scenarios that have been envisioned for the EIC, 10 ps TOF would enable 3 sigma pi/K and K/p separation at 3.5 and 6 GeV/c in the barrel. For the forward (hadron) direction, at a distance of 3m, one could achieve 6.5 and 11 GeV/c separation, respectively. TOF, in conjunction with a TPC, would aid in electron identification. It would also provide a start counter for DIRC detectors which require timing (aka, TOP detectors). TOF may provide a more cost-effective and compact solution compared to other technologies.

2.5.1 Past

### 2.5.1.1 What was planned for this period?

Our group proposed to have built and tested a digitizer board based on the DRS4 ASIC. This board, when coupled with the fast preamp (UFAMP) we built previously under the EIC R&D program, and read out with the PHENIX MPC-EX FEM, would serve as the prototype for the full electronics system for a 10 picosecond timing system at the EIC. It would prove that a scalable, low power, high resolution (<10 ps) electronics system could be built that would be capable of handling 15 kHz DAQ rates with 4 us trigger latency. This kind of system does not currently exist today. We also planned to study the UV behavior of the ANL 6 cm^2 MCP-PMT with the fused silica window (the first ever in existence).

2.5.1.2 What was achieved?

We were not funded for the electronics development as proposed, and the advice from the

committee strongly suggested that we needed to look in more detail into determining how well the start time can be determined at the EIC. We thus started some long overdue simulation studies on this matter. Note that one clear solution would be to have full coverage, 4π, TOF, where one can then readily determine the start time by measuring the TOF of the electron track and the electron's path length. Here we study what happens for a limited acceptance TOF covering the central barrel only ($|\eta|<1.1$).

For this study, DIS events are generated using PYTHIA 6.428, and particles coming from the vertex in the TOF acceptance are smeared with resolutions of dt = 10 ps, dp/p = 2%, and dL = 1 mm. A start time t_{start} for each of the N particles in the TOF acceptance is determined using t_{det} - $t_{start} = t_{flight} = (L/c)[1+(m/p)^2]^{1/2}$, where t_{det} is the measured time in the TOF detector and L is the path length from the vertex to the detector. Since a priori we don't know the particle type and hence the mass m to use, we use a brute force technique by trying every possible type. We assume that electrons and muons can be rejected, so we only take pions, kaons and protons as possible particle types. For N particles, there will be 3^N possible combinations, and each of these possible combinations will have a set of N start times, one from each particle. From these 3^N combinations we select the one with the least variance in the t_{start}, i.e., we select the PID combination which gives the best agreement on the start time between the N particles. We find that this criterion determines the right PID combination 99% of the time. A best self-determined start time is then calculated by the weighted sum of the t_{start} from the N tracks. In fig. 2.5.1 we show the distribution for this self-determined start time minus the true start time for N=2 tracks, as well as the start time resolution vs the number of tracks N. Even for just 2 tracks in the TOF, one can determine a very good start time with a resolution of 6.3 ps.
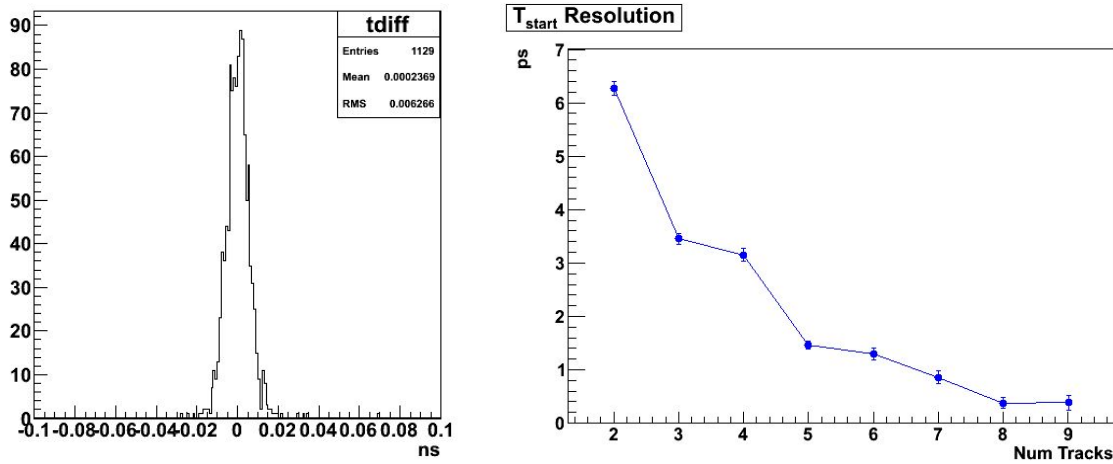
Figure 2.5.1: The distribution of the self-determined start time minus the true start time for 2 tracks in the TOF (left), and the start time resolution vs the number of tracks in the TOF (right)

The above simulation is done from pure PYTHIA6 events only, and not from running the events through an experiment Monte Carlo. It thus does not include many experimental effects which might impact the above resolution. A TOF system has recently been implemented in the

sPHENIX simulation in order to fully explore the experimental details of 10 picosecond TOF at an EIC detector. Some other questions to explore in the simulation beyond the start time are what level of momentum and path length resolution are tolerable for a 10 ps detector, what segmentation will be required, the rate capability needed, etc.

2.5.1.3 What was not achieved, why not, and what will be done to correct it?

Not much progress has been made on the digitizer board since there was no funding for the board fabrication and stuffing. Discussions are currently underway with Nu Xu of LBNL, Jianping Chen of JLab, and a group of Chinese universities (CCNU, USTC, Tsinghua U) to form an R&D Consortium to develop 10-20 ps mRPC TOF detectors for use in sPHENIX, SoLID, and the EIC. We hope that funding from this group will be available sometime in 2017 to support the production of the digitizer board.

The study of the ANL UV-sensitive MCP-PMT has been delayed at BNL since the UV laser lab was busy doing SiPM and LXe drift calibration studies for the NEXO experiment. We are scheduled to start our studies early in the next calendar year.

2.5.2 Future

2.5.2.1 What is planned for the next funding cycle and beyond? How, if at all, is this planning different from the original plan?

We plan to continue testing the digitizer board, as well as the much thinner alternative dielectric versions of the mRPC. We also plan a test beam at Fermilab, and to continue lab studies of different mRPC designs. Initial tests of the timing resolution of the ANL UV MCP-PMT have not been as expected, and we hope that over the next 6 months we can determine what the impediments to getting the expected timing resolution are.

2.5.2.2 What are the critical issues?

We believe that the main impediment to faster development is the lack of dedicated labor to this project. With the ending of the funding this past fiscal year for our UIUC post-doc, we have lost a major component of the most productive labor for our R&D. It cannot be stated enough that having a good person working on your project is the single best determinant of success. Currently we have funding for summer undergraduate students from ACU and Howard. Our group is supplementing this with an undergraduate SULI student working at BNL with Mickey in the spring.

3. Photosensors and Electronics

3.1 Summary

The main objective of this R&D effort during the proposed funding period was to continue to identify and assess suitable photosensor and electronics solutions for the readout of the EIC Cherenkov detectors, both for the full EIC detector and for prototypes in beam tests. Within the main objective, one of the goals was to identify a cost-efficient, and eventually common, readout solution that is shared within the EIC-PID consortium. Ultimately, in the long term, this R&D work will allow us to make a recommendation about the best photosensors and electronics solutions for the PID detectors in EIC implementation.

3.2 Sensors in High-B Fields

3.2.1 Past

3.2.1.1 What was planned for this period?

In this reporting period we planned to measure the gain of Photonis (25-μm pore size) and Hamamatsu (10-μm pore size) multi-anode MCP PMTs as a function of B, and θ.

3.2.1.2 What was achieved?

In Summer 2016 the gain of Hamamatsu (10-μm pore size) multi-anode MCP PMT was measured as a function of B and $\theta=0°$, $10°$. The results are shown in Fig.3.2.1. The data were
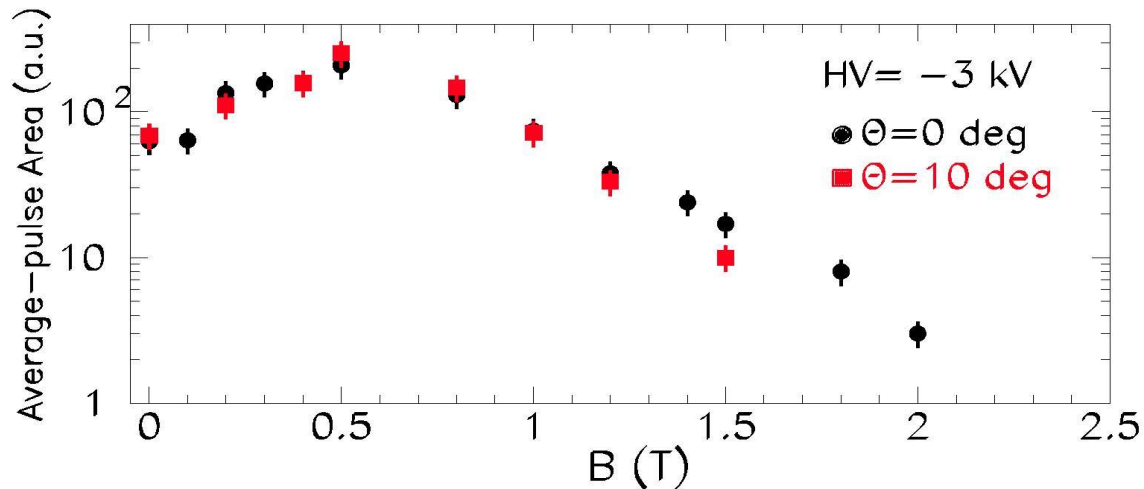
Figure 3.2.1: Average-pulse area of Hamamatsu (10-μm pore size) R10754-07-M16 MCP PMT as a function of magnetic-field magnitude. θ is the angle between the normal to the PMT front and the B-field vector. Above fields of 0.5 T, the gain at θ=10° decreases faster with B than at 0°, which narrows the maximum field at which the sensor can be operated at this orientation. The error bars show preliminary 20% uncertainties dominated by systematics.

obtained by illuminating only two detector channels. The gain increases at small field magnitudes and reaches a maximum at 0.5 T for both test orientations. Above 0.5 T the gain decreases exponentially as the B-field increases, however the decrease is faster at 10° than at 0°. The high voltage on the PMT at which the tests were done was 94% of the maximum recommended value. The voltage across the gap between the two micro-channel plates was 96% of its maximum value, whereas the voltages across the micro-channel plates themselves were 90% of their maximum values. The PMT gain is expected to be affected most by a HV increase across these three stages when compensating for the magnetic-field effect. Thus, our measurements were at the limit of the ability to compensate for gain decrease by HV increase.

The gain of Photonis (25-µm pore size) was measured as a function of B for $\theta = 0°$ and $10°$. The results are shown in Fig. 3.2.2. The maximum field at which we obtained viable signals from the
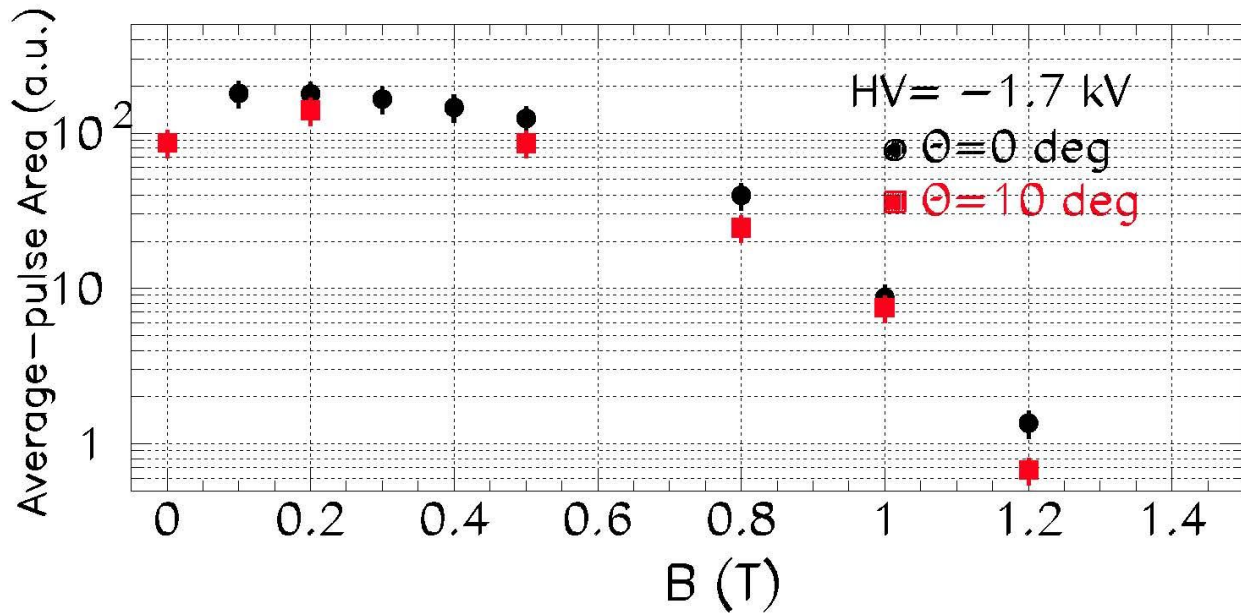
Figure 3.2.2: Average-pulse area of Planacon (25-µm pore size) XP85012 MCP PMT as a function of magnetic-field magnitude. θ is the angle between the normal to the PMT front and the B-field vector. Overall, at all fields the gain at θ=10° is lower than at 0°. At both orientations the maximum field at which we readout viable signals was 1.2 T. The error bars show preliminary 20% uncertainties dominated by systematics.

PMT was 1.2 T. Our data show that sensors with such a large pore size are not adequate to use in the expected field of 1.5 – 3 T of an EIC detector. The main purpose of the Planacon evaluation was to pave the way for future loans from Photonis of a 10-µm pore size sample(s) for detailed evaluations.

With respect to the upgrade of the JLab test setup to allow for timing measurements (that is planned for 2017), C. Hyde was successful to negotiate funds from ODU to purchase an appropriate laser. We will build an optics box for the laser and commission the system in 2017.

3.2.2 Future

3.2.2.1 What is planned for the next funding cycle and beyond? How, if at all, is this planning different from the original plan?

For the rest of 2017 we plan to (a) evaluate the gain of Planacon (10-µm pore size) multi-anode MCP PMTs as a function of (B, θ, φ, HV), (b) implement a timing upgrade to the test facility, and (c) begin setting up an MCP-PMT simulation. This plan does not differ from the original plan in terms of content. Due to restricted budget, some of the activities may not be completed in 2017.

3.2.2.2 What are the critical issues?

The availability of R&D funding at the beginning of the calendar year is critical in order to keep this program within the planned timelines.

3.3 LAPPDs

The LAPPD™ project is a multi-year project involving a number of institution, with a goal to create an MCP-PMT that has the same very high performance as existing MCP-PMTs, but at a significantly lower cost. While the commercial LAPPD MCP-PMT's are promising, the design needs to be optimized for EIC PID applications.

3.3.1 Past

3.3.1.1 What was planned for this period?

For FY2017, we planned to further study the UV-sensitive MCP-PMT and then concentrate on providing a small format (6cm x 6cm active area) micro-channel plate (MCP) photodetectors with pad readout for characterization by the collaboration. Included in this work will be a pad readout for improved rate capability and possible physical spacing variations of the MCPs to improve magnetic field performance.

3.3.1.2 What was achieved?

In summer 2016, experiment data from the FTBF beamline experiment on MCP-PMTs was further analyzed in details. The study was done using the 120 GeV proton beam, the beam spot size is about 8 mm^2, and the intensity was varied to achieve fluxes from 3.3-150 KHz/cm^2. Fig. 3.3.1 shows the gain dependence of the flux rate. The gain of the tested MCP-PMT keeps no obvious variation until the rate reaches 75 KHz/cm^2, indicating good rate capability tolerance up to 75 KHz/cm^2. This rate capability is above the EIC requirement.
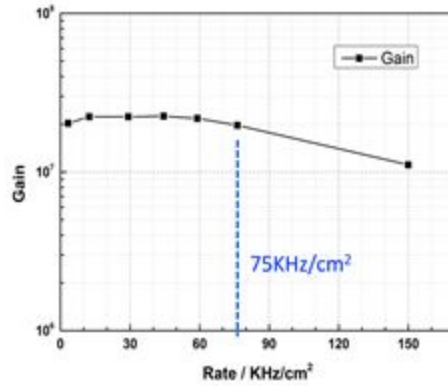
Figure 3.3.1: MCP-PMT gain dependence of flux rate. The rate capability of the tested MCP-PMT is up to 75 KHz/cm^2, above the EIC requirement.

The detector production work is concentrated on the design and fabrication of pixelated MCP-PMTs to fulfill the large demand of pixelated readout for various applications. A new pad readout was designed based on the dimension of the stripline readout assembly. Fig. 3.3.2 shows the designed pad readout assembly. The base assembly is made out of a complete ceramic block. The empty area was directly cut down so that frit sealing between the base and side wall is omitted. There are pads on both inside and outside surfaces of the base, and they are connected through vias. For the 1st version of this pixelated readout, we designed it to be 5 mm x 5 mm with 0.5 mm spacing for the inside surface and 3 mm x 3 mm with 2.5 mm spacing for the outside surface. This kind of design exactly fits the Belle II upgrade requirement, and is easier to be fabricated in the company. Currently, the version-1 pixelated base assembly is under fabrication by a company. For the 2nd version of this pixelated readout, the pixel size will be reduced to 2.25 mm x 2.25 mm with 0.5 mm spacing for the inside surface to fulfill the EIC RICH detector requirement.
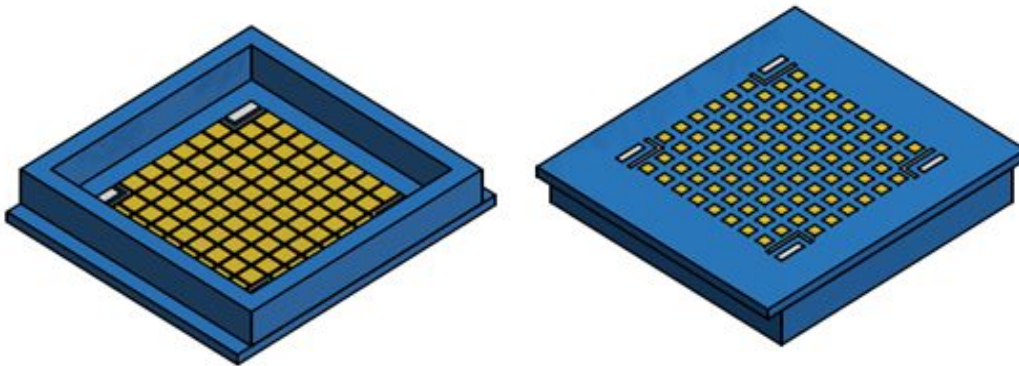
Figure 3.3.2: Design of the pixelated base assembly with 5mm x 5mm pad size and 0.5 mm spacing for the inside surface.

Besides the pad-to-pad readout through vias, we also built a chamber for the study of possibility of pad readout induced by capacitive coupling. The chamber is completed at Argonne and ready for testing.
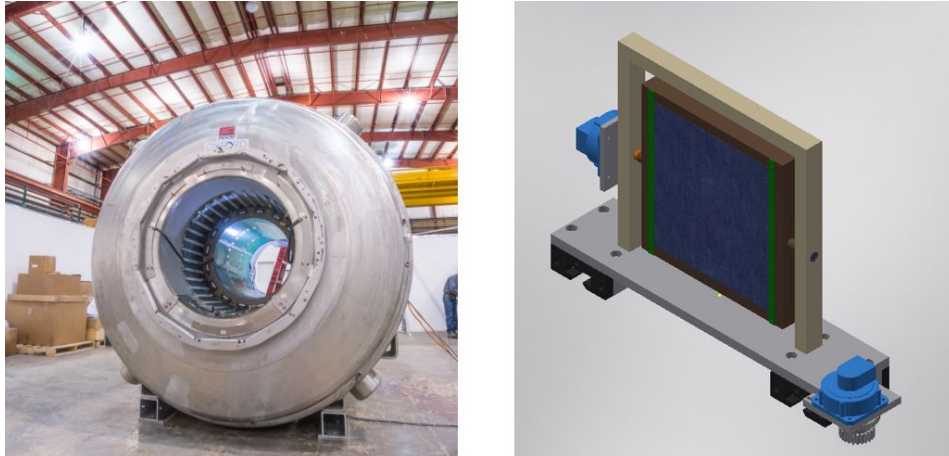
Figure 3.3.3: (left) View of the test solenoid facility in the high-bay area at Argonne Bldg. 366. (right) Self-designed test stand for 20 cm x 20 cm MCP magnetic field performance testing.

Part of the effort at Argonne was supported by Argonne LDRD to build a magnetic test facility for MCP-PMTs, especially for 20 cm x 20 cm LAPPD testing. At Argonne, a solenoid magnetic facility was acquired for calibration of the magnetic field for G-2 experiment. The solenoid facility can be used as a general magnetic field testing facility in the future. We designed a transporter with the capability of testing MCP-PMTs up to 20 cm x 20 cm. All components of this holder are made of non-magnetic materials, the router can be electrically controlled and the MCP-PMT center is aligned with the center of the magnetic facility. The solenoid facility and the designed transporter is shown in Fig 3.3.3. The transporter is currently under fabrication at the ANL mechanical shop.

3.3.2 Future

3.3.2.1 What is planned for the next funding cycle and beyond? How, if at all, is this planning different from the original plan?

In the rest of FY2017, we plan to continue MCP-PMT fabrication and characterization work as scheduled:

- Produce version-1 pad readout MCP-PMT after obtain the pixelated base.
- Produce a modified MCP-PMT with smaller gap between two MCPs for testing.
- Explore the possibility of pad readout induced by capacitive coupling.
- Obtain version-2 pad readout base assembly.

- Complete the ANL magnetic field testing facility.
- Test the newly produced MCP-PMTs.

3.3.2.2 What are the critical issues?

Loss of funding support is the major issue for the ANL MCP-PMT project. The project was previously funded through DOE-HEP detector R&D funding. From FY17, the Office of HEP at DOE has determined to winding down the support of LAPPD project since Incom. Inc has started the pilot production and commercialization of LAPPD. This reduced ~ 1M funding support for the ANL-LAPPD project. The optimization of LAPPD MCP-PMTs is now supported by fractional funding from Argonne LDRD, US-Japan Belle II and EIC detector R&D funding to keep the program ongoing at a minimum spending.

3.4 Readout Sensors and Electronics for Detector Prototypes

3.4.1 Past

The data acquisition system for the first mRICH beam test was provided by the INFN group led by Marco Contalbrigo. There were four Hamamatsu H12700A modules mounted at the sensor plane. The H12700A readout consisted of three circuit boards as described in http://infn.fe.infn.it/~mcontalb/JLAB12/RICH_midterm_review/RICH_Electronics_Turisini.pdf. The adapter board is a passive board mounting connectors to couple the MA-PMTs socket to the electronics. The ASIC board is based on the MAROC3 chip by OMEGA described in http://omega.in2p3.fr/index.php/download-center/doc_details/393-proceedingsieeenss2010maroc3.html served by voltage regulators, e.g. AD5620 by Analog Devices. The FPGA board is based on the Xilinx Artix7 and uses the Finisar FTE8510N1LCN optical transceiver to connect to a N-GXE-LC-01 fiber gigabit Ethernet to PCI express bus adapter in the readout computer.

The electronics for DIRC beam tests at CERN were mostly provided by the PANDA DIRC group at GSI (although some items were also procured by the EIC R&D program for the DIRC R&D prior to formation of the eRD14 consortium).

3.4.2 Future

3.4.2.1 What is planned for the next funding cycle and beyond? How, if at all, is this planning different from the original plan?

The consortium is developing of a strategy for to provide photosensors for future R&D needs to reduce cost and maximize synergies. As suggested by the committee, the plan will be presented in the FY18 funding proposal and will involve continued work with the INFN group - but will also include the Hawaii group responsible, among other things, for providing the electronics for the Belle II TOP DIRC and KLM detectors.

4. Manpower

Abilene Christian University

Rusty Towell, Faculty, 25% of time spent on project

Matt Kimball, Haley Stien, Aric Tate, Cecily Towell, undergraduate, 0.25 FTE, summer research at BNL, supervised by R. Towell and M. Chiu

Argonne National Laboratory

Bob Wagner, Staff Scientist, 10% of time spent on project, No FTE

Lei Xia, Staff Scientist, 15% of time spent on project, No FTE

Junqi Xie, Staff Scientist, 25% of time spent on project, 0.14 FTE

Jingbo Wang, Postdoctoral Appointee, 25% of time spent on project, 0.25 FTE

Tim Cundiff, Engineer, 10% of time spent on project, 0.07 FTE

Brookhaven National Laboratory

Mickey Chiu, Staff Scientist, 40% of time spent on project

Andrey Sukhanov, Electronics Engineer, 0.10 FTE

Rob Pisani, Scientific Associate, 0.25 FTE

Catholic University of America

Grzegorz Kalicy, Faculty, 50% of research time on project

Duke University

Zhiwen Zhao, Research professor

Georgia State University

Xiaochun He, faculty, 30% of time spent on project.

Cheuk-Ping Wong, PhD graduate student, 100% of time on the project, located at Georgia State University, supervised by X. He.

Reid Simpson, undergraduate student, 20% of time on the project.

Sawaiz Syed, temp research staff, 50% of time on the project (mechanical and electrical design), located at Georgia State University, supervised by X. He.

GSI Helmholtzzentrum für Schwerionenforschung GmbH

Roman Dzhygadlo, Postdoctoral Research Associate, 25% of time spent on project

Carsten Schwarz, Staff Scientist, 15% of time spent on project

Jochen Schwiening, Senior Staff Scientist, 15% of time spent on project

Howard University

Marcus Alfred, Faculty, 25% of time spent on project

John Blakley, Kahlil Dixon, Robert Neblett, undergraduate, 0.25 FTE, summer research at BNL, supervised by M. Alfred and M. Chiu

Jefferson Lab

Carl Zorn, Staff Scientist

Los Alamos

Hubert van Hecke, Staff Scientist

Old Dominion University

Charles Hyde, Faculty, 30% of research time on project

Lee Allison, Doctoral Student, 100% on project. Located at ODU/JLab and supervised by C. Hyde and G. Kalicy

Stony Brook University

Pawel Nadel-Turonski, Adjunct Professor, 30% of research time spent on project

University of Illinois at Urbana-Champaign

Matthias Grosse-Perdekamp, Faculty, 10% of time spent on project

University of South Carolina

Yordanka Ilieva, Faculty, 30% of time spent on project

Alessio DelDotto, Postdoctoral Fellow, 100% of time spent on project

Corinne Barber, Undergraduate Student, 17% of time spent on project (8 weeks), located at Jefferson Lab, supervised by Y. Ilieva, C. Zorn, and K. Park

Colin Gleason, Graduate Student, 5% of time spent on project (2 weeks), located at Jefferson Lab, supervised by Y. Ilieva

Include a list of the existing manpower and what approximate fraction each has spent on the project. If students and/or postdocs were funded through the R&D, please state where they were located and who supervised their work.

5. External Funding

ANL

- ANL-LDRD project: A Strategic Scientific Program to establish Argonne Leadership in the Development of the Future Electron-Ion Collider, Oct 1, 2016 – Sep 30, 2017: 80K

- US-Japan Belle II: Oct 1, 2016 – Apr 30, 2017: 44K

ODU

- University funds for fast (picosecond) laser pulser procurement for High-B timing measurements: $15k.
- University funds for travel for CERN PS test beam, Oct 10 - Nov 3, 2016: $4k.
- DOE Grant funding for Graduate Research Assistant, 100% on project: $19,000 (including indirect costs), 1 July 2016 — 31 December 2017

GSU

- University funds provided the major portion of the support for a graduate student and the research staff.

GSI

- Mechanical components for the 2016 DIRC prototype: $3k.
- Travel for DIRC prototype beam test at CERN PS, Oct 10 - Nov 3, 2016: $22k.

INFN-Ferrara

- Development of higher density readout electronics moving towards the compatibility with 3 mm sensors (such as the ones required for the mRICH prototype): $6.5k.

See also the respective sections for more details on TOF, photosensors, etc.

6. Publications

6.1 In Preparation

C.P. Wong *et al*., Modular Focusing Ring-Imaging Cherenkov Detector for Electron-Ion Collider Experiments, to be submitted to NIM A.

6.2 Published or Submitted

A. Deldotto et al.: Design and R&D of RICH detectors for EIC experiments, poster at RICH2016 (9th International Workshop on Ring Imaging Cherenkov Detectors), September 5-9, 2016, Bled, Slovenia, submitted to Nucl. Instrum. Meth. A.

L. Allison: High-performance DIRC detector for use in an Electron-Ion Collider, Proceedings for ICHEP2016 (38th International Conference on High Energy Physics), August 3-10, 2016, Chicago, IL, submitted to Proceedings of Science.

G. Kalicy: PID systems for the JLab EIC full-acceptance detector, Proceedings for ICHEP2016 (38th International Conference on High Energy Physics), August 3-10, 2016, Chicago, IL, submitted to Proceedings of Science.

G. Kalicy et al.: DIRC detector for the future Electron Ion Collider experiment; Proceedings of the DIRC2015 Workshop, 11-13 November, Giessen, Germany, Journal of Instrumentation, Volume 11, March 2016.

Y. Ilieva et al.: MCP-PMT studies at the High-B test facility at Jefferson Lab; Proceedings of the DIRC2015 Workshop, 11-13 November, Giessen, Germany; Journal of Instrumentation, Volume 11, March 2016.

R. Dharmapalan et al: MCP-based photodetectors for cryogenic applications, Journal of Instrumentation, 11, C02019 (2016).

J. Xie et al.: Development of a low-cost fast-timing microchannel plate photodetector; Nucl. Instrum. Meth. A 824 (2016) 159-161.

J. Wang et al.: Development and testing of cost effective, 6cm×6cm MCP-based Photodetectors for fast timing applications; Nucl. Instrum. Meth. A 804 (2015) 84.

J. Xie et al. (LAPPD collaboration): Design and fabrication of prototype 6×6 cm2 microchannel plate photodetector with bialkali photocathode for fast timing applications, Nucl. Instrum. Meth. A 784 (2015) 242.